An efficient method for simultaneously reconstructing Robin coefficient and heat flux in an elliptic equation using an MCGM

TALAAT ABDELHAMID
Physics and Mathematical Engineering Dep.
Faculty of Electronic Engineering
Menoufya University
EGYPT
talaat.2008@yahoo.com

OLATUNJI MUMINI OMISORE
Shenzhen Institutes of Advanced Tech.
Chinese Academy of Sciences
Shenzhen 518055
CHINA
omisore@siat.ac.cn

Abstract: A modified conjugate gradient method (MCGM) is proposed for simultaneously reconstructing Robin coefficient and heat flux in an elliptic system from a single part of the boundary measurements of the solution. The simultaneous identification problem is formulated as a constrained optimization problem using the output least squares method with Tikhonov regularization. The differentiability and adjoint equations are investigated for finding the gradient formulas and determining the step lengths, respectively. Finite element method is employed to discretize the constrained optimization problem which reduced to a sequence of unconstrained optimization problem by adding the regularization term. Some comparisons are presented with the Levenberg-Marquardt method proposed by [1]. Numerical examples investigate the efficiency and accuracy of the proposed algorithm.

Key-Words: Simultaneous identification, Numerical reconstruction, Heat flux and Robin coefficient, Tikhonov's regularization, FEM, MCGM.

1 Introduction

Ill-posed inverse problem of reconstructing Robin coefficient and heat flux from transient temperature histories measured in the heat conduction problems and stationary diffusion equations are constantly of a great interest during three last decades. A literature review and a presentation of different method is presented in [2, 3, 4, 5, 6, 7] and the references therein. Several numerical methods are proposed for the Robin inverse problems in the context of corrosion detection [8, 9, 10]. [11] employed the nonlinear CGM for reconstructing the Robin coefficient with Laplace equation and noted that the convergence was relatively slowly. Also, used preconditioning technique using Hilbert space scales and Sobolev gradients for accelerating its convergence but did not test it numerically. [12] introduced an application of conjugate gradient method for estimation of the wall heat flux of a supersonic combustor. [13, 14] introduced the mathematical and numerical justification for the reconstruction of only one parameter Robin coefficient of the inverse problem using the nonlinear conjugate gradient method.

One of the advantages of the finite element method as compared with the finite difference method are that complicated geometry, general boundary conditions and variable or non-linear material properties can be manipulated relatively easily [15, 16, 13, 17]. The finite element method has a solid theoretical foundation which gives added reliability and in many cases is able to mathematically analyze and estimate the error in the approximate finite element solution [18]. [1] studied numerically the simultaneous identification of Robin coefficient and heat flux using surrogate functional and Levenberg-Marquardt method. Moreover, there is a little work in the literature on simultaneous reconstructing Robin coefficient and heat flux using a modified conjugate gradient method (MCGM) and comparison between the two methods are the focus of this work.

The reset of this paper is organized as follows: Sections 2 is devoted to describe the variational formulation for the elliptic problem and stability of the optimization problem. Section 3 briefly derives the partial Fréchet derivatives of the forward solution to obtain the gradient of the Robin coefficient and heat flux also introduces the adjoint equations to find a simple explicit expressions to simplify computing the minimization equation. Section 4 introduces the finite element approximation and its convergence. Section 5 discusses the numerical algorithm using a modified conjugate gradient method (MCGM). Section 6 introduces some numerical experiments to present the efficiency, accuracy, and robustness of the proposed method for simultaneously reconstructing Robin coefficient and heat flux in the optimization problem. Some comparisons presented to illustrate the efficiency of the proposed modified conjugate gradient method (MCGM) comparing with Levenberg-Marquardt method.

2 Mathematical formulation

Consider an elliptic system which occupies an open, bounded, and connected polyhedral domain $\Omega \subset R^2$ with the boundaries $\Gamma_i (i = 1, 2, 3)$ which can be modeled by the following elliptic equation:

$$\begin{cases} -\nabla \cdot (\alpha(\mathbf{x})\nabla u) + c(\mathbf{x})u = f(\mathbf{x}) & \text{in } \Omega, \\ \alpha(\mathbf{x})\frac{\partial u}{\partial n} + \gamma(\mathbf{x})u(\mathbf{x}) = g(\mathbf{x}) & \text{on } \Gamma_1, \\ \alpha(\mathbf{x})\frac{\partial u}{\partial n} = q(\mathbf{x}) & \text{on } \Gamma_2, \\ \alpha(\mathbf{x})\frac{\partial u}{\partial n} = 0 & \text{on } \Gamma_3. \end{cases} \tag{2.1}$$

Hence $\alpha(\mathbf{x})$ is the heat conductivity and a smooth boundary $\partial\Omega$ consists of three parts i.e. $\partial\Omega = \Gamma_1 \cup \Gamma_2 \cup \Gamma_3$ is a finite collection of disjoint, smooth $(d-1)$-dimensional polyhedral domain. The functions $\alpha(\mathbf{x})$ and $c(\mathbf{x})$ are the heat conductivity and radiation which be constraint by $0 < \alpha_1 < \alpha(\mathbf{x}) < \alpha_2$ and $0 < c_1 < c(\mathbf{x}) < c_2$, respectively. The parameters identification problem $\gamma(\mathbf{x})$ and $q(\mathbf{x})$ are contained in the following constrained sets: $K_\gamma = \{\gamma(\mathbf{x}) \in L^2(\Gamma_1) : 0 < \gamma_1 \leq \gamma(\mathbf{x}) \leq \gamma_2, \text{ a.e. on } \Gamma_1\}$, and $K_q = \{q(\mathbf{x}) \in L^2(\Gamma_2) : 0 < q_1 \leq q(\mathbf{x}) \leq q_2, \quad \text{a.e. on } \Gamma_2\}$. Such that (x, y) denoted by $\mathbf{x}$. Let u solve system (2.1) and Let $u(\mathbf{x}) = z^\delta$ on Γ_3 where z^δ is the measurement data of the exact solution u, the parameter δ is used here to emphasize the existence of the noise in the measured data.

This paper aims to justify numerically the validation and effectiveness of the regularization formulation for solving the ill-posed inverse problem of the two parameters Robin coefficient on Γ_1 and heat flux on Γ_2 reconstruction. In addition, we will solve the nonlinear finite element minimization problem by using a modified conjugate gradient method for simultaneously reconstructing the Robin coefficient and heat flux.

Now, we formulate the considered parameters identification problem as a constrained minimizing process

$$\begin{aligned} \min_{(\gamma,q)\in K_\gamma \times K_q} J(\gamma, q) &= \|u(\gamma, q) - z^\delta\|^2_{\Gamma_3} + \beta\|\gamma\|^2_{\Gamma_1} \\ &+ \eta\|q\|^2_{\Gamma_2}, \end{aligned} \tag{2.2}$$

where $(\gamma, q) \in K_\gamma \times K_q$ and $u \equiv u(\gamma, q)(\mathbf{x}) \in H^1(\Omega)$ satisfies

$$\begin{aligned} \int_\Omega a\nabla u \cdot \nabla v dx + \int_\Omega cuv dx + \int_{\Gamma_1} \gamma uv ds = \int_\Omega f v dx \\ + \int_{\Gamma_1} gv ds + \int_{\Gamma_2} qv ds \;\; \forall \;\; v \in H^1(\Omega). \end{aligned} \tag{2.3}$$

Note that (2.3) is the variational formulation associated with the elliptic problem (2.1). For any $(\gamma, q) \in K_\gamma \times K_q$ there exists a unique solution $u(\gamma, q) \in H^1(\Omega)$ to (2.1)(see, Theorem 2.1 [1]).

To deal with the instability of the inverse problem, we reformulate it as a constrained minimization problem (2.2) where $u(\gamma, q)$ solves the variational formulation (2.3). We assume that, β and η are the regularization parameters. Furthermore, $\gamma \in L^\infty(\Gamma_1)$ in the admissible set K_γ which replaced by $\gamma \in L^2(\Gamma_1) \cap L^\infty(\Gamma_1)$. Suppose that $\|\cdot\|_{H^1(\Gamma_1)}$ is defined by

$$\|v\|^2_{H^1(\Gamma_1)} = \|\nabla v\|^2_{L^2(\Omega)} + \|v\|^2_{L^2(\Gamma_1)},$$

which equivalent to the standard norm $\|\cdot\|_{H^1(\Omega)}$.

Theorem 2.1. *There exists at least one minimizer to the optimization problem (2.2).*

Proof. Clearly, $\inf J(\gamma, q)$ is a finite over the admissible set $K_\gamma \times K_q$, and thus there exists a minimizing sequence $(\gamma^n, q^n) \in K_\gamma \times K_q$ such that

$$\lim_{n\to\infty} J(\gamma^n, q^n) = \inf_{(\gamma,q)\in K_\gamma \times K_q} J(\gamma, q). \tag{2.4}$$

Using Banach-Alaoglu theorem, the boundedness of the sequence γ^n in $L^\infty(\Gamma_1)$ and q^n in $L^\infty(\Gamma_2)$ implies that there exists a subsequence, still denoted by $\{(\gamma^n, q^n)\}$, and some $(\gamma^*, q^*) \in K_\gamma \times K_q$ such that

$$(\gamma^n, q^n) \rightharpoonup (\gamma^*, q^*) \text{ weak convergence in } K_\gamma \times K_q,$$

Using (2.4), the strong convergence of u^n in $L^2(\partial\Omega)$, and lower semicontinuity imply that

$$\begin{aligned} J(\gamma^*, q^*) &= \|u(\gamma^*, q^*) - z^\delta\|^2_{\Gamma_3} + \beta\|\gamma^*\|^2_{\Gamma_1} \\ &+ \eta\|q^*\|^2_{\Gamma_2}, \\ &= \lim_{n\to\infty} \|u(\gamma^n, q^n) - z^\delta\|^2_{\Gamma_3} + \beta\|\gamma^*\|^2_{\Gamma_1} \\ &+ \eta\|q^*\|^2_{\Gamma_2}, \\ &\leq \lim_{n\to\infty} \|u(\gamma^n, q^n) - z^\delta\|^2_{\Gamma_3} \\ &+ \beta \lim_{n\to\infty} \inf \|\gamma^n\|^2_{\Gamma_1} + \eta \lim_{n\to\infty} \inf \|q^n\|^2_{\Gamma_2}, \\ &\leq \lim_{n\to\infty} \inf J(\gamma^n, q^n) \\ &= \inf_{(\gamma,q)\in K_\gamma \times K_q} J(\gamma, q). \end{aligned} \tag{2.5}$$

Which implies that (γ^*, q^*) is a minimizer of the functional (2.2). ☐

The stability property of the optimization problem with respect to the observation errors z^δ and the sequence $\{(\gamma^n, q^n)\}$ of the minimizers has a subsequence weak convergence in $K_\gamma \times K_q$ (see, Theorem 3.2 [1]).

3 Differentiability results for the sensitivity and adjoint equations

In this section, we introduce the sensitivity problems and establish the differentiability of the solution $u(\gamma, q)$ with respect to the heat f ux $q(\mathbf{x})$ and Robin coeff cient $\gamma(\mathbf{x})$. We suppose that the Robin coeff cient $\gamma(\mathbf{x})$ is perturbed by a small amount $\gamma(\mathbf{x}) + \lambda$, and the heat f ux $q(\mathbf{x})$ perturbed by $q(\mathbf{x}) + \xi$, such that λ and ξ any directions in $L^\infty(\Gamma_1)$ and $L^\infty(\Gamma_2)$, respectively:

$$u(\gamma(\mathbf{x})+\lambda, q) \approx u(\gamma, q)+u'_\gamma(\gamma, q)\lambda+\mathcal{O}(\|\lambda\|^2_{L^\infty(\Gamma_1)}),$$

and

$$u(\gamma(\mathbf{x}), q+\xi) \approx u(\gamma, q)+u'_q(\gamma, q)\xi+\mathcal{O}(\|\xi\|^2_{L^\infty(\Gamma_2)}).$$

Then replacing γ in the direct problem by $\gamma(\mathbf{x}) + \lambda$, and $u(\gamma, q)$ by $u(\gamma(\mathbf{x}) + \lambda, q)$, subtracting from the forward problem (2.1), neglecting the second order terms as well as $q(\mathbf{x})$ are all similarly, we obtain

$$\begin{cases} -\nabla\cdot(\alpha(\mathbf{x})\nabla(u'_\gamma(\gamma, q)\lambda)) + c(\mathbf{x})(u'_\gamma(\gamma, q)\lambda) = 0 \\ \text{in } \Omega, \\ \alpha(\mathbf{x})\frac{\partial(u'_\gamma(\gamma,q)\lambda)}{\partial n} + \gamma(\mathbf{x})(u'_\gamma(\gamma, q)\lambda) = -\lambda u(\gamma, q) \\ \text{on } \Gamma_1, \\ \alpha(\mathbf{x})\frac{\partial(u'_\gamma(\gamma,q)\lambda))}{\partial n} = 0 \text{ on } \Gamma_2, \\ \alpha(\mathbf{x})\frac{\partial(u'_\gamma(\gamma,q)\lambda))}{\partial n} = 0 \text{ on } \Gamma_3, \end{cases}$$

and

$$\begin{cases} -\nabla\cdot(\alpha(\mathbf{x})\nabla(u'_q(\gamma, q)\xi)) + c(\mathbf{x})(u'_q(\gamma, q)\xi) = 0 \\ \text{in } \Omega, \\ \alpha(\mathbf{x})\frac{\partial(u'_q(\gamma,q)\xi)}{\partial n} + \gamma(\mathbf{x})(u'_q(\gamma, q)\xi) = 0 \\ \text{on } \Gamma_1, \\ \alpha(\mathbf{x})\frac{\partial(u'_q(\gamma,q)\xi))}{\partial n} = \xi \text{ on } \Gamma_2, \\ \alpha(\mathbf{x})\frac{\partial(u'_q(\gamma,q)\xi))}{\partial n} = 0 \text{ on } \Gamma_3, \end{cases}$$

which are linear with respect to λ and ξ, respectively.

Lemma 3.1. *For any $(\gamma, q) \in K_\gamma \times K_q$ and the solution $u(\gamma, q)$ is differentiable with respect to (γ, q) in the sense that*

$$\frac{\|u(\gamma+\lambda, q) - u(\gamma, q) - u'_\gamma(\gamma, q)\lambda\|_{H^1(\Omega)}}{\|\lambda\|_{L^\infty(\Gamma_1)}} \to 0 \quad \text{as } \lambda \to 0 \text{ in } L^\infty(\Gamma_1), \tag{3.1}$$

and

$$\frac{\|u(\gamma, q+\xi) - u(\gamma, q) - u'_q(\gamma, q)\xi\|_{H^1(\Omega)}}{\|\xi\|_{L^\infty(\Gamma_2)}} \to 0 \quad \text{as } \xi \to 0 \text{ in } L^\infty(\Gamma_2). \tag{3.2}$$

Proof. We assume the function $w \equiv u(\gamma + \lambda, q) - u(\gamma, q) - u'_\gamma(\gamma, q)$ which satisf es

$$\begin{cases} -\nabla\cdot(\alpha\nabla w) + cw = 0 & \text{in } \Omega, \\ \alpha\frac{\partial w}{\partial n} + \gamma w = -\lambda(u(\gamma+\lambda, q) - u(\gamma, q)) & \text{on } \Gamma_1, \\ \alpha\frac{\partial w}{\partial n} = 0 & \text{on } \Gamma_2, \\ \alpha\frac{\partial w}{\partial n} = 0 & \text{on } \Gamma_3, \end{cases} \tag{3.3}$$

we obtain the variational form

$$\int_\Omega \alpha|\nabla w|^2 dx + \int_\Omega c|w|^2 dx + \int_{\Gamma_1} \gamma|w|^2 ds = -\int_{\Gamma_1} \lambda(u(\gamma+\lambda, q) - u(\gamma, q))w ds. \tag{3.4}$$

By using Sobolev trace theorem, we derive

$$\|w\|_{H^1(\Omega)} \le C\|\lambda\|_{L^\infty(\Gamma_1)}\|u(\gamma+\lambda, q)-u(\gamma, q)\|_{H^1(\Omega)}. \tag{3.5}$$

Also, by replacing $u(\gamma, q)$ by $u(\gamma+\lambda, q)$ into (2.1), we obtain

$$\begin{aligned} &\int_\Omega \alpha|\nabla(u(\gamma+\lambda, q) - u(\gamma, q))|^2 dx \\ &+ \int_\Omega c|(u(\gamma+\lambda, q) - u(\gamma, q))|^2 dxnb \\ &+ \int_{\Gamma_1} \gamma|(u(\gamma+\lambda, q) - u(\gamma, q))|^2 ds \\ = &-\int_{\Gamma_1} \lambda u(\gamma+\lambda, q)(u(\gamma+\lambda, q) - u(\gamma, q))ds. \end{aligned} \tag{3.6}$$

Using Sobolev trace theorem, we obtain

$$\begin{aligned} &\|u(\gamma+\lambda, q) - u(\gamma, q)\|^2_{H^1(\Omega)} \\ &+\|u(\gamma+\lambda, q) - u(\gamma, q)\|^2_{L^2(\Gamma_1)} \\ &\le C\|\lambda\|_{L^\infty(\Gamma_1)}\|u(\gamma+\lambda, q)\|_{H^1(\Omega)} \\ &\quad \|u(\gamma+\lambda, q) - u(\gamma, q)\|_{L^2(\Omega)}. \end{aligned} \tag{3.7}$$

Then,

$$\|u(\gamma+\lambda,q)-u(\gamma,q)\|_{H^1(\Omega)} \leq C\|\lambda\|_{L^\infty(\Gamma_1)}\|u(\gamma+\lambda,q)\|_{H^1(\Omega)}. \quad (3.8)$$

The proof of Theorem 2.1 indicates that $\|\lambda\|_{L^\infty(\Gamma_1)}$ is suff ciently small and $\|u(\gamma+\lambda,q)\|_{H^1(\Omega)}$ is uniformly bounded. Thus, it follows that

$$\frac{\|u(\gamma+\lambda,q)-u(\gamma,q)-u_\gamma^{'}(\gamma,q)\lambda\|_{H^1(\Omega)}}{\|\lambda\|_{L^\infty(\Gamma_1)}} \to 0 \quad \text{as } \lambda \to 0 \text{ in } L^\infty(\Gamma_1). \quad (3.9)$$

Similarly, for $u(\gamma,q+\xi)$ we deduce that (3.2) is valid. □

From the proof of the Lemma 3.1, we have the following expansion:

$$u(\gamma+\lambda,q)=u(\gamma,q)+u_\gamma^{'}(\gamma,q)\lambda+\mathcal{O}(\|\lambda\|^2_{L^\infty(\Gamma_1)}),$$

and

$$u(\gamma,q+\xi)=u(\gamma,q)+u_q^{'}(\gamma,q)\xi+\mathcal{O}(\|\xi\|^2_{L^\infty(\Gamma_2)}).$$

We introduce the adjoint equations for the previous partial derivatives equations which be associated to $u(\gamma,q)$ in any direction $d\equiv(u-z^\delta)|_{y=1}\in L^2(\Gamma_3)$, and $p\equiv(u-z^\delta)|_{x=0}\in L^2(\Gamma_3)$. We def ne $u_\gamma^{'}(\gamma,q)^*d$ and $u_q^{'}(\gamma,q)^*p$ by solving the following systems

$$\begin{cases} -\nabla\cdot(\alpha(\mathbf{x})\nabla(u_\gamma^{'}(\gamma,q)^*d))+c(\mathbf{x})(u_\gamma^{'}(\gamma,q)^*d)=0 \\ \text{in } \Omega, \\ \alpha(\mathbf{x})\frac{\partial(u_\gamma^{'}(\gamma,q)^*d)}{\partial n}+\gamma(\mathbf{x})(u_\gamma^{'}(\gamma,q)^*d)=0 \\ \text{on } \Gamma_1, \\ \alpha(\mathbf{x})\frac{\partial(u_\gamma^{'}(\gamma,q)^*d))}{\partial n}=0 \text{ on } \Gamma_2, \\ \alpha(\mathbf{x})\frac{\partial(u_\gamma^{'}(\gamma,q)^*d))}{\partial n}=-d \text{ on } \Gamma_3, \end{cases}$$

and

$$\begin{cases} -\nabla\cdot(\alpha(\mathbf{x})\nabla(u_q^{'}(\gamma,q)^*p))+c(\mathbf{x})(u_q^{'}(\gamma,q)^*p)=0 \\ \text{in } \Omega, \\ \alpha(\mathbf{x})\frac{\partial(u_q^{'}(\gamma,q)^*p)}{\partial n}+\gamma(\mathbf{x})(u_q^{'}(\gamma,q)^*p)=0 \\ \text{on } \Gamma_1, \\ \alpha(\mathbf{x})\frac{\partial(u_q^{'}(\gamma,q)^*p))}{\partial n}=0 \text{ on } \Gamma_2, \\ \alpha(\mathbf{x})\frac{\partial(u_q^{'}(\gamma,q)^*p))}{\partial n}=p \text{ on } \Gamma_3. \end{cases}$$

Theorem 3.1. *The objective functional $J(\gamma,q)$ is Fréchet differentiable and its Fréchet derivative is $\frac{\partial J(\gamma,q)}{\partial\gamma}$, $\gamma\in K_\gamma$ in the direction λ and Fréchet derivative $\frac{\partial J(\gamma,q)}{\partial q}$ with respect to $q\in K_q$ in the direction ξ are given by*

$$\frac{\partial J}{\partial\gamma}[\lambda]=2\int_{\Gamma_1}\lambda[u(\gamma,q)(u_\gamma^{'}(\gamma,q)^*d)+\beta\gamma]ds, \quad (3.10)$$

and

$$\frac{\partial J}{\partial q}[\xi]=2\int_{\Gamma_2}\xi[(u_q^{'}(\gamma,q)^*p)+\eta q]ds. \quad (3.11)$$

Proof. From Lemma 3.1, noting that

$$\|u_\gamma^{'}(\gamma,q)\lambda\|_{H^1(\Omega)}\leq C\|\lambda\|_{L^\infty(\Gamma_1)}$$

and

$$\|u_q^{'}(\gamma,q)\xi\|_{H^1(\Omega)}\leq C\|\xi\|_{L^\infty(\Gamma_2)},$$

we have

$$\min_{(\gamma,q)\in K_\gamma\times K_q} J_0(\gamma,q)=\int_{\Gamma_3}(u(\gamma,q)-z^\delta)^2ds. \quad (3.12)$$

Then, we derive

$$\begin{aligned} J_0(\gamma+\lambda,q)-J_0(\gamma,q) &= \int_{\Gamma_3}(u(\gamma+\lambda,q)-z^\delta)^2ds \\ &\quad -\int_{\Gamma_3}(u(\gamma,q)-z^\delta)^2ds, \\ &= \int_{\Gamma_3}(u(\gamma,q)+u_\gamma^{'}(\gamma,q)\lambda+\mathcal{O}(\|\lambda\|^2_{L^\infty(\Gamma_1)})-z^\delta)^2ds \\ &\quad -\int_{\Gamma_3}(u(\gamma,q)-z^\delta)^2ds, \\ &= 2\int_{\Gamma_3}(u(\gamma,q)-z^\delta)u_\gamma^{'}(\gamma,q)\lambda+\mathcal{O}(\|\lambda\|^2_{L^\infty(\Gamma_1)})ds \\ &\quad +2\int_{\Gamma_3}(u_\gamma^{'}(\gamma,q)\lambda+\mathcal{O}(\|\lambda\|^2_{L^\infty(\Gamma_1)}))^2ds, \\ &= 2\int_{\Gamma_3}(u(\gamma,q)-z^\delta)u_\gamma^{'}(\gamma,q)\lambda ds+\mathcal{O}(\|\lambda\|^2_{L^\infty(\Gamma_1)}). \end{aligned}$$

Then, we obtain

$$\frac{\partial J_0}{\partial\gamma}[\lambda]=2\int_{\Gamma_3}(u(\gamma,q)-z^\delta)(u_\gamma^{'}(\gamma,q)\lambda)ds. \quad (3.13)$$

Similarly, the Fréchet derivative of J_0 with respect to q in the direction ξ shows that

$$\frac{\partial J_0}{\partial q}[\xi]=2\int_{\Gamma_3}(u(\gamma,q)-z^\delta)(u_q^{'}(\gamma,q)\xi)ds. \quad (3.14)$$

By taking $\varphi = u_\gamma^{'}(\gamma, q)\lambda$, $\psi = u_\gamma^{'}(\gamma, q)^* d$, and multiplying (3.1) by ψ and (3.10) by φ, then we apply Green's second identity by subtracting the two equations

$$0 = \int_\Omega \{\psi\nabla\cdot(\alpha\nabla\varphi) - \varphi\nabla\cdot(\alpha\nabla\psi)\}\, dx$$
$$= \int_{\partial\Omega} \left(\alpha\frac{\partial\varphi}{\partial n}\psi - \alpha\frac{\partial\psi}{\partial n}\varphi\right) ds. \quad (3.15)$$

By substituting the boundary conditions for φ and ψ, we obtain

$$\int_{\Gamma_1} \lambda u(\gamma, q)\psi ds = \int_{\Gamma_3} d\varphi ds. \quad (3.16)$$

Taking $\tilde{\varphi} = u_q^{'}(\gamma, q)\xi$, $\tilde{\psi} = u_q^{'}(\gamma, q)^* p$, and multiplying (3.1) by $\tilde{\psi}$ and (3.10) by $\tilde{\varphi}$, then we apply Green's second identity

$$0 = \int_\Omega \left\{\tilde{\psi}\nabla\cdot(\alpha\nabla\tilde{\varphi}) - \tilde{\varphi}\nabla\cdot(\alpha\nabla\tilde{\psi})\right\} dx$$
$$= \int_{\partial\Omega} \left(\alpha\frac{\partial\tilde{\varphi}}{\partial n}\tilde{\psi} - \alpha\frac{\partial\tilde{\psi}}{\partial n}\tilde{\varphi}\right) ds. \quad (3.17)$$

By substituting the boundary conditions for $\tilde{\varphi}$ and $\tilde{\psi}$, we obtain

$$\int_{\Gamma_2} \xi\tilde{\psi} ds = \int_{\Gamma_3} p\tilde{\varphi} ds. \quad (3.18)$$

By substituting from (3.16) into (3.13), we deduce

$$\frac{\partial J}{\partial\gamma}[\lambda] = 2\int_{\Gamma_1} \lambda \left[u(\gamma, q)(u_\gamma^{'}(\gamma, q)^* d) + \beta\gamma\right] ds, \quad (3.19)$$

such that

$$\frac{\partial J_0}{\partial\gamma}[\lambda] = 2\int_{\Gamma_1} \lambda u(\gamma, q)(u_\gamma^{'}(\gamma, q)^* d) ds.$$

Similarly, the Fréchet derivative of J_0 with respect to q in the direction ξ, we obtain

$$\frac{\partial J}{\partial q}[\xi] = 2\int_{\Gamma_2} \xi \left[(u_q^{'}(\gamma, q)^* p) + \eta q\right] ds, \quad (3.20)$$

and

$$\frac{\partial J_0}{\partial q}[\xi] = 2\int_{\Gamma_2} \xi(u_q^{'}(\gamma, q)^* p) ds.$$

This completes the proof of Theorem 3.1. □

Remark 3.1. *The idea of the conventional gradient* $\frac{\partial J}{\partial q}$ *and* $\frac{\partial J}{\partial\gamma}$ *are the* $L^2(\Gamma_2)$ *and* $L^2(\Gamma_1)$ *gradient respectively. which can be defined as follows:*

$$\frac{\partial J}{\partial q}[\xi] = \int_{\Gamma_2} \xi\frac{\partial J}{\partial q} ds \ \ and \ \ \frac{\partial J}{\partial\gamma}[\lambda] = \int_{\Gamma_1} \lambda\frac{\partial J}{\partial\gamma} ds.$$

such that the integral refers to duality between $L^\infty(\Gamma_2)$ *and its dual* $\left(L^2(\Gamma_2)\right)'$ *for the heat flux* q. *and* $\frac{\partial J}{\partial q}$ *is an element in the dual space* $\left(L^2(\Gamma_2)\right)'$. *According to the Robin coefficient on the boundary* Γ_1 *is same. The gradient is used to update an element in the admissible set* K_q *and* K_γ.

4 Methodology of the finite element technique

Finite element method is a powerful tool and an effective numerical technique for partial differential equations in engineering and many fields. The fact that modern engineers can obtain detailed information about the structure, thermal, electromagnetic problems with virtual experiments largely gives credit finite element method. Now, we apply the finite element approximation method for solving the continuous minimization problem (2.2). We triangulate the polyhedral domain Ω with a regular triangulation $\mathcal{T}^h$ of a simplicial elements. Then we define the linear finite element space V_h by

$$V_h = \{\phi_h \in C(\Omega) : \phi_h|_{\mathcal{T}_i} \in \tilde{F}(\mathcal{T}_i)\ \forall\ \mathcal{T}_i \in \mathcal{T}_h\},$$

such that $\tilde{F}(\mathcal{T}_i)$ denotes the space of linear polynomials on the elements $\mathcal{T}_i$. We define a restrictions of the space V_h are $V_{\Gamma_1}^h$ and $V_{\Gamma_2}^h$ on Γ_1 and Γ_2 respectively. Also, the discrete admissible sets K_γ^h and K_q^h defined as follows

$$K_\gamma^h = \{\gamma_h \in V_{\Gamma_1}^h : \gamma_1 \le \gamma_h(x) \le \gamma_2\ \forall\ x \in \Gamma_1\},$$

and

$$K_q^h = \{q_h \in V_{\Gamma_2}^h : q_1 \le q_h(x) \le q_2\ \forall\ x \in \Gamma_2\},$$

where $K_\gamma^h \subset K_\gamma$ and $K_q^h \subset K_q$, we approximate the optimization problem (2.2) by the following discrete minimization system

$$\min_{(\gamma_h, q_h)\in K_\gamma^h\times K_2^h} J_h(\gamma_h, q_h) = \int_{\Gamma_3} (u_h(\gamma_h, q_h) - z^\delta)^2 ds$$
$$+\beta\int_{\Gamma_1} \gamma_h^2 ds + \eta\int_{\Gamma_2} q_h^2 ds, \quad (4.1)$$

where the function $u_h(\gamma_h, q_h) \in V^h$ satisfies the weak formulation

$$\int_\Omega \alpha\nabla u_h\cdot\nabla v_h dx + \int_\Omega c u_h v_h dx + \int_{\Gamma_1} \gamma_h u_h v_h ds$$
$$= \int_\Omega f v_h dx + \int_{\Gamma_1} g v_h ds + \int_{\Gamma_2} q_h v_h ds\ \ \forall\ v_h \in V^h. \quad (4.2)$$

In the following analysis, we need the standard interpolation operator $I_h : W^{1,\infty}(\Omega) \to v_h$ and the projection operator $Q_h : H^1(\Omega) \to v_h$ is defined as

$$\int_\Omega \nabla Q_h w \cdot \nabla v_h dx + \int_{\partial\Omega} Q_h w v_h ds = \int_\Omega \nabla w \cdot \nabla v_h dx + \int_{\partial\Omega} w v_h ds \quad \forall\ w \in H^1(\Omega)\ \ v_h \in V_h. \tag{4.3}$$

Then, for any $p > d = dim(\Omega)$, we have

$$\lim_{h\to 0} \|I_h w - w\|_{W^{1,\infty}(\Omega)} = 0\ \ \forall\ \ w \in W^{1,\infty}(\Omega),$$

and

$$\lim_{h\to 0} \|Q_h w - w\|_{H^1(\Omega)} = 0\ \ \forall\ \ w \in H^1(\Omega).$$

The following theorem shows the existence of the minimizer for the finite element discretization problem (4.1).

Theorem 4.1. *There exists at least one minimizer to the finite element problem (4.1).*

Proof. Such that $\min J_h(\gamma_h, q_h)$ is a finite over the admissible set $K^h_\gamma \times K^h_q$. Hence, there exists a minimizing sequence $\{(\gamma_h, q_h)\} \in K^h_\gamma \times K^h_q$ such that

$$\lim_{n\to\infty} J_h(\gamma^n_h, q^n_h) = \min_{(\gamma_h,q_h)\in K^h_\gamma \times K^h_q} J_h(\gamma_h, q_h).$$

The uniform boundedness of $\{(\gamma_h, q_h)\}$ in $K^h_\gamma \times K^h_q$ and the norm equivalence in the finite dimensional space implies that there exists a subsequence denoted by $\{(\gamma^n_h, q^n_h)\}$ and some $\{(\gamma^*_h, q^*_h)\}$ in $K^h_\gamma \times K^h_q$ such that

$$\{(\gamma^n_h, q^n_h)\} \rightharpoonup (\gamma^*_h, q^*_h)\ \text{ in }\ K^h_\gamma \times K^h_q,\ \ n \to \infty.$$

Now, we prove that (γ^*_h, q^*_h) is a minimizer of (4.1). From the definition of $u_h(\gamma^n_h, q^n_h)$ and $u_h(\gamma^*_h, q^*_h)$, we have

$$\int_\Omega \alpha \nabla u_h(\gamma^n_h, q^n_h) \cdot \nabla v_h dx + \int_\Omega c u_h(\gamma^n_h, q^n_h) v_h dx + \int_{\Gamma_1} \gamma^n_h u_h(\gamma^n_h, q^n_h) v_h ds = \int_\Omega f v_h dx + \int_{\Gamma_1} g v_h ds + \int_{\Gamma_2} q^n_h v_h ds\ \ \forall\ \ v_h \in V^h, \tag{4.4}$$

and

$$\int_\Omega \alpha \nabla u_h(\gamma^*_h, q^*_h) \cdot \nabla v_h dx + \int_\Omega c u_h(\gamma^*_h, q^*_h) v_h dx + \int_{\Gamma_1} \gamma^*_h u_h(\gamma^*_h, q^*_h) v_h ds = \int_\Omega f v_h dx + \int_{\Gamma_1} g v_h ds + \int_{\Gamma_2} q^*_h v_h ds\ \ \forall\ \ v_h \in V^h. \tag{4.5}$$

By taking $v_h = u_h(\gamma^n_h, q^n_h)$ into (4.4), we see that

$$\|u_h(\gamma^n_h, q^n_h)\|_{H^1(\Omega)} \le C,$$

where C is a constant independent on n and h. By subtracting equation (4.5) from (4.4) and assume that $w^n_h \equiv u_h(\gamma^n_h, q^n_h) - u_h(\gamma^*_h, q^*_h)$ gives

$$\int_\Omega \alpha \nabla w^n_h \cdot \nabla v_h dx + \int_\Omega c w^n_h v_h dx + \int_{\Gamma_1} \left(\gamma^n_h u_h(\gamma^n_h, q^n_h) - \gamma^*_h u_h(\gamma^*_h, q^*_h)\right) v_h ds = \int_{\Gamma_2} \left(q^n_h - q^*_h\right) v_h ds, \tag{4.6}$$

we can rewrite it as following

$$\int_\Omega \alpha \nabla w^n_h \cdot \nabla v_h dx + \int_\Omega c w^n_h v_h dx + \int_{\Gamma_1} \gamma^n_h w^n_h v_h ds = -\int_{\Gamma_1} (\gamma^n_h - \gamma^*_h) u_h(\gamma^*_h, q^*_h) v_h ds + \int_{\Gamma_2} (q^n_h - q^*_h) v_h ds. \tag{4.7}$$

Then, taking $v_h = w^n_h$ and using the Cauchy- Schwarz inequality, and the lower bound of the above assumptions, we derive

$$\alpha_0 \|\nabla w^n_h\|^2_{L^2(\Omega)} + c_0 \|w^n_h\|^2_{L^2(\Omega)} + \gamma_0 \|w^n_h\|^2_{L^2(\Gamma_1)} \le \|\gamma^n_h - \gamma^*_h\|_{L^\infty(\Gamma_1)} \|u_h(\gamma^*_h, q^*_h)\|_{L^2(\Gamma_1)} \|w^n_h\|_{L^2(\Gamma_1)} + \|q^n_h - q^*_h\|_{L^2(\Gamma_2)} \|w^n_h\|_{L^2(\Gamma_2)}. \tag{4.8}$$

Hence the norm equivalence in the finite dimensional spaces implies that $w^n_h \to 0$ (i.e., $u_h(\gamma^n_h, q^n_h) \to u_h(\gamma^*_h, q^*_h)$ in $H^1(\Omega)$ as $k \to \infty$).

Consequently, we have

$$\begin{aligned} J_h(\gamma_h^*, q_h^*) &= \int_{\Gamma_3} (u_h(\gamma_h^*, q_h^*) - z^\delta)^2 ds ds \\ &+ \beta \int_{\Gamma_1} (\gamma_h^*)^2 + \eta \int_{\Gamma_2} (q_h^*)^2 ds \\ &\leq \lim_{n\to\infty} \int_{\Gamma_3} (u_h(\gamma_h^n, q_h^n) - z^\delta)^2 ds \\ &+ \beta \lim_{n\to\infty} \inf \int_{\Gamma_1} \gamma_h^{n2} ds \\ &+ \eta \lim_{n\to\infty} \inf \int_{\Gamma_2} q_h^{n2} ds \\ &\leq \lim_{n\to\infty} \inf \left\{ \int_{\Gamma_3} (u_h(\gamma_h^n, q_h^n) - z^\delta)^2 ds \right. \\ &\left. + \beta \int_{\Gamma_1} \gamma_h^{n2} ds + \eta \int_{\Gamma_2} q_h^{n2} ds \right\} \\ &= \lim_{n\to\infty} \inf J_h(\gamma_h^n, q_h^n) \\ &= \min_{(\gamma_h, q_h) \in K_\gamma^h \times K_q^h} J_h(\gamma_h, q_h). \end{aligned} \quad (4.9)$$

This show that $(\gamma_h^*, q_h^*) \in K_\gamma^h \times K_q^h$ is a minimizer of the discrete optimization problem (4.1). □

Lemma 4.1. *Let $\{(\gamma_h, q_h)\} \in K_\gamma^h \times K_q^h$ be weak convergence to $(\gamma^*, q^*) \in K_\gamma \times K_q$ as $h \to 0$, then there exists a subsequence which denoted by $\{(\gamma_h, q_h)\}$, such that*

$$u_h(\gamma_h, q_h) \to u(\gamma^*, q^*) \;\; in \;\; L^2(\Gamma_3) \;\; as \;\; h \to 0,$$

which implies that

$$\lim_{n\to\infty} \int_{\Gamma_3} (u(\gamma_h, q_h) - z_h^\delta)^2 ds = \int_{\Gamma_3} (u(\gamma^*, q^*) - z^\delta)^2 ds.$$

Proof. Let $v_h = u_h$ into (4.2), we obtain

$$\begin{aligned} \int_\Omega \alpha |\nabla u_h|^2 dx + \int_\Omega c|u_h|^2 dx + \int_{\Gamma_1} \gamma_h |u_h|^2 ds \\ = \int_\Omega f u_h dx + \int_{\Gamma_1} g u_h ds + \int_{\Gamma_2} q_h u_h ds \\ \forall \;\; v_h \in V^h. \end{aligned} \quad (4.10)$$

Then $\|u_h(\gamma_h, q_h)\|_{H^1(\Omega)} \leq C$ is bounded and C is constant not depend on h. There exists a convergent subsequence, still denoted by $u_h(\gamma_h, q_h)$, such that

$$u_h(\gamma_h, q_h) \to u^* \;\; weakly \;\; in \;\; H^1(\Omega) \;\; as \;\; h \to 0.$$

From the compactness results, this implies

$$u_h(\gamma_h, q_h) \to u^* \;\; strongly \;\; in \;\; L^2(\Gamma_3) \;\; as \;\; h \to 0.$$

We show that $u^* \equiv u(\gamma^*, q^*)$. For any $v \in H^1(\Omega)$, let $v_h = Q_h v$ be a test function, obtain that

$$\begin{aligned} \int_\Omega \alpha \nabla u_h \cdot \nabla v_h dx + \int_\Omega c u_h v_h dx + \int_{\Gamma_1} \gamma_h u_h v_h ds \\ = \int_\Omega f v_h dx + \int_{\Gamma_1} g v_h ds + \int_{\Gamma_2} q_h v_h ds \\ \forall \, v_h \in V^h, \end{aligned} \quad (4.11)$$

such that

$$\begin{aligned} \int_\Omega \alpha \nabla u_h \cdot \nabla v_h dx &= \int_\Omega \alpha \nabla u_h \cdot \nabla v dx \\ &+ \int_\Omega \alpha \nabla u_h \cdot \nabla (v_h - v) dx, \\ \int_\Omega c u_h v_h dx &= \int_\Omega c u^* v dx + \int_\Omega c u_h (v_h - v) dx \\ &+ \int_\Omega c(u_h - u^*) v dx, \\ \int_{\Gamma_1} \gamma_h u_h v_h ds &= \int_{\Gamma_1} \gamma_h u^* v ds + \int_{\Gamma_1} \gamma_h u_h (v_h - v) ds \\ &+ \int_{\Gamma_1} \gamma_h (u_h - u^*) v ds, \\ \int_\Omega f v_h dx &= \int_\Omega f v dx + \int_\Omega f (v_h - v) dx. \end{aligned}$$

By the convergence of $v_h = Q_h v$, $u_h(\gamma_h, q_h)$ weak convergence in $H^1(\Omega)$, and (γ_h, q_h) weak convergence in $K_\gamma^h \times K_q^h$ as $h \to 0$, we derive

$$\begin{aligned} \int_\Omega \alpha \nabla u^* \cdot \nabla v dx + \int_\Omega c u^* v dx + \int_{\Gamma_1} \gamma^* u^* v ds \\ = \int_\Omega f v dx + \int_{\Gamma_1} g v ds + \int_{\Gamma_2} q^* v ds. \end{aligned} \quad (4.12)$$

Then we conclude that $u^* \equiv u(\gamma^*, q^*)$. □

The following lemma we will need illustrates the density result. It has been proved in [13].

Lemma 4.2. $C^\infty(\Omega)$ *is weak $*$ dense in* $L^\infty(\Omega)$.

For any $\chi \in L^\infty(\Omega)$, there exists an $\chi^n \in C^\infty(\Omega)$ such that

$$\int_\Omega \chi^n \varphi dx \to \int_\Omega \chi \varphi dx \;\; \forall \varphi \in L^1(\Omega), \;\; n \to \infty.$$

The following theorem shows that the convergence of the finite element solution to the minimizer of the continuous optimization problem.

Theorem 4.2. *Let $\{(\gamma_h^*, q_h^*)\}$ be a sequence of minimizers to the discrete minimization problem (4.1). Then each subsequence of $\{(\gamma_h^*, q_h^*)\}$ has a subsequence converging to a minimizer of the continuous optimization problem(2.2).*

Proof. From the uniform boundedness of γ_h^* in $L^\infty(\Gamma_1)$ and q_h^* in K_2 implies that there exists a subsequence, also denoted by $\{(\gamma_h^*, q_h^*)\}$, and some $\{(\gamma^*, q^*)\}$ such that

$$\gamma_h^* \to \gamma^* \quad weak * in \;\; L^\infty(\Gamma_1) \;\; as \;\; h \to 0,$$

$$q_h^* \to q^* \quad weak * in \;\; L^\infty(\Gamma_2) \;\; as \;\; h \to 0,$$

and Lemma 4.1 implies that

$$u_h(\gamma_h^*, q_h^*) \to u(\gamma^*, q^*) \;\; in \;\; L^2(\Gamma_3).$$

For any $(\gamma, q) \in K_\gamma \times K_q$ and let $\varepsilon > 0$, from Lemma 4.2 there exists a $(\gamma^\varepsilon, q^\varepsilon) \in C^\infty(\Gamma_1) \times C^\infty(\Gamma_2)$ such that

$$(\gamma^\varepsilon, q^\varepsilon) \to (\gamma, q) \;\; weak \; in \; K_\gamma \times K_q.$$

For any $(\gamma^\varepsilon, q^\varepsilon) \in K_\gamma \times K_q$, let $(\gamma_h^\varepsilon, q_h^\varepsilon) = (Q_h\gamma^\varepsilon, Q_h q^\varepsilon) \in K_\gamma^h \times K_q^h$. The property of interpolation operator Q_h implies that

$$\lim_{h\to 0} \|u_h(\gamma_h^\varepsilon, q_h^\varepsilon) - u(\gamma, q)\|_{L^2(\Gamma_3)} = 0.$$

We derive that (γ_h^*, q_h^*) is the minimizer of J over $K_\gamma^h \times K_q^h$

$$\begin{aligned}
J_h(\gamma_h^*, q_h^*) &= \int_{\Gamma_3} (u_h(\gamma_h^*, q_h^*) - z^\delta)^2 ds + \beta \int_{\Gamma_1} (\gamma_h^*)^2 ds \\
&+ \eta \int_{\Gamma_2} (q_h^*)^2 ds, \\
&\le \int_{\Gamma_3} (u_h(\gamma_h^\varepsilon, q_h^\varepsilon) - z^\delta)^2 ds + \beta \int_{\Gamma_1} (\gamma_h^\varepsilon)^2 ds \\
&+ \eta \int_{\Gamma_2} (q_h^\varepsilon)^2 ds, \\
&= J_h(\gamma_h^\varepsilon, q_h^\varepsilon) = J_h(Q_h\gamma^\varepsilon, Q_h q^\varepsilon). \qquad (4.13)
\end{aligned}$$

Then from Lemma 4.1 and the convergence property of the interpolation operator Q_h

$$\begin{aligned}
J(\gamma^*, q^*) &= \int_{\Gamma_3} (u(\gamma^*, q^*) - z^\delta)^2 ds + \beta \int_{\Gamma_1} (\gamma^*)^2 ds \\
&+ \eta \int_{\Gamma_2} (q^*)^2 ds, \\
&\le \lim_{h\to 0} \int_{\Gamma_3} (u_h(\gamma_h^*, q_h^*) - z^\delta)^2 ds \\
&+ \lim_{h\to 0} \inf[\beta \int_{\Gamma_1} (\gamma_h^*)^2 ds + \eta \int_{\Gamma_2} (q_h^*)^2 ds], \\
&\le \lim_{h\to 0} \inf J_h(\gamma_h^*, q_h^*), \\
&\le \lim_{h\to 0} \inf J_h(Q_h\gamma^\varepsilon, Q_h q^\varepsilon), \\
&\le \int_{\Gamma_3} (u_h(\gamma^\varepsilon, q^\varepsilon) - z^\delta)^2 ds + \beta \int_{\Gamma_1} (\gamma^\varepsilon)^2 ds \\
&+ \eta \int_{\Gamma_2} (q^\varepsilon)^2 ds. \qquad (4.14)
\end{aligned}$$

By assuming $\varepsilon \to 0$, we obtain

$$J(\gamma^*, q^*) \le J(\gamma, q) \;\; \forall \;\; (\gamma, q) \in K_\gamma \times K_2,$$

which indicates that (γ^*, q^*) is a minimizer of the functional $J(\gamma, q)$. □

5 Numerical algorithm using an M-CGM

In this section, we describe the MCGM for the numerical solution of the minimization problem to identify the two parameters Robin coeff cient and heat f ux, simultaneously. Each iteration requires solving two sensitivity and two adjoint equations to compute the gradient formulas with respect to γ and q. The idea of the modif cation in CGM is summarized as follows: The given initial guess (γ^0, q^0) helps for computing the heat f ux q^{k+1} (i.e., q^{k+1} computed by (γ^k, q^k)), while the heat transfer coeff cient γ^{k+1} is computed by (γ^k, q^{k+1}) as shown in the following algorithm. MCGM stops when the reconstructions are accurate enough or satisfy the stopping criteria.

Algorithm 5.1.

a- Choose the initial guess (γ^0, q^0), directions (d_q^0, d_γ^0), and set $k := 0$.

b- Solve the forward problem (2.1) $u(\gamma^k, q^k)$ and compute the residual r_q^k

$$r_q^k = u(\gamma^k, q^k) - z^\delta \quad on \;\; \Gamma_3.$$

c- Solve the adjoint equation (3.10)

d- Determine the gradient $\frac{\partial J(\gamma^k,q^k)}{\partial q}$ *such that*

$$\frac{\partial J(\gamma^k,q^k)}{\partial q} = 2(u_q^{'}(\gamma^k,q^k)^* p + \eta q^k).$$

e- The conjugate coefficient β_q^k *is given by*

$$\beta_q^k = \frac{\|\partial J(\gamma^k,q^k)/\partial q\|^2_{L^2(\Gamma_2)}}{\|\partial J(\gamma^{k-1},q^{k-1})/\partial q\|^2_{L^2(\Gamma_2)}}.$$

f- Compute the descent direction with respect to $q(x,y)$

$$d_q^{k+1} = -\frac{\partial J(\gamma^k,q^k)}{\partial q} + \beta_q^k d_q^k.$$

g- Solve the sensitivity equation $u_q^{'}(\gamma^k,q^k)\xi$ *in (3.1).*

h- Compute the step length α_q^k

$$\alpha_q^k = -\frac{\langle r_k, u_q^{'}(\gamma^k,q^k,d_q^{k+1})\rangle_{L^2(\Gamma_3)} + \eta\langle q^k, d_q^{k+1}\rangle_{L^2(\Gamma_2)}}{\|u_q^{'}(\gamma^k,q^k,d_q^{k+1})\|^2_{L^2(\Gamma_3)} + \eta\|d_q^{k+1}\|^2_{L^2(\Gamma_2)}}. \tag{5.1}$$

i- Update the heat flux $q(x,y)$ *by*

$$q^{k+1} = q^k + \alpha_k d_q^{k+1}.$$

j- Solve the forward problem (2.1) $u(\gamma^k,q^{k+1})$ *and compute* r_γ^k

$$r_\gamma^k = u(\gamma^k,q^{k+1}) - z^\delta \quad on \ \ \Gamma_3.$$

k- Solve the adjoint problem $u_\gamma^{'}(\gamma^k,q^{k+1})^* d$ *in (3.10)*

l- Determine the gradient $\frac{\partial J(\gamma^k,q^{k+1})}{\partial \gamma}$ *such that*

$$\frac{\partial J(\gamma^k,q^{k+1})}{\partial \gamma} = 2(u(\gamma^k,q^{k+1})(u_\gamma^{'}(\gamma^k,q^{k+1})^* d) + \beta\gamma^k).$$

m- The conjugate coefficient β_γ^k *given by*

$$\beta_\gamma^k = \frac{\|\partial J(\gamma^k,q^{k+1})/\partial \gamma\|^2_{L^2(\Gamma_1)}}{\|\partial J(\gamma^{k-1},q^{k+1})/\partial \gamma\|^2_{L^2(\Gamma_1)}}.$$

n- Compute the descent direction for $\gamma(x,y)$

$$d_\gamma^k = -\frac{\partial J(\gamma^k,q^{k+1})}{\partial \gamma} + \beta_q^k d_q^k.$$

o- Solve the sensitivity equation $u_\gamma^{'}(\gamma^k,q^{k+1})\lambda$ *in (3.1).*

p- Compute α_γ^k

$$\alpha_\gamma^k = -\frac{\langle r_k, u_\gamma^{'}(\gamma^k,q^{k+1},d_\gamma^{k+1})\rangle_{L^2(\Gamma_3)} + \beta\langle \gamma^k, d_\gamma^{k+1}\rangle_{L^2(\Gamma_1)}}{\|u_\gamma^{'}(\gamma^k,q^{k+1},d_\gamma^{k+1})\|^2_{L^2(\Gamma_3)} + \beta\|d_\gamma^{k+1}\|^2_{L^2(\Gamma_1)}}. \tag{5.2}$$

q- Update the Robin coefficient γ^k *by*

$$\gamma^{k+1} = \gamma^k + \alpha_\gamma^k d_\gamma^{k+1}.$$

r- If $\frac{\|q^{k+1}-q^k\|_{L^2(\Gamma_2)}}{\|q^k\|_{L^2(\Gamma_2)}} \le \varepsilon_1$*, and* $\frac{\|\gamma^{k+1}-\gamma^k\|_{L^2(\Gamma_1)}}{\|\gamma^k\|_{L^2(\Gamma_1)}} \le \varepsilon_2$ *Stop; otherwise* $k := k+1$*, and go to Step 2.*

The step lengths α_q^k and α_γ^k are determined by the quadratic approximation of a two-variable functional. By using the mean value theorem and Taylor expansion, we can derive the forward operator $u(\gamma,q)$ with respect to γ, and q as shown in equations (5.1) and (5.2) to determine the step lengths α_q^k and α_γ^k, respectively. For determining the step lengths α_q^k and α_γ^k, this requires solving two auxiliary and adjoint equations for every iteration. The considered numerical examples in the present study and previous studies of inverse problems [19, 13] prove that the step lengths work very well.

6 Numerical experiments and discussions

In this section, we will execute the proposed algorithm 5.1 to simultaneously reconstruct the parameters heat f ux and Robin coeff cient in the optimization problem (2.1). The considered solution domain Ω is a rectangular as $\Omega = (0,1)\times(0,2)$ which discretized using triangular mesh such that each small rectangular is divided to two triangles as a f nite element triangulation. We have the domain boundary consists of three parts $\Gamma_1 = \{(x,y) : x = 1, \quad 0 \le y \le 2\}$, $\Gamma_2 = \{(x,y) : y = 0, \quad 0 \le x \le 1\}$, and $\Gamma_3 = \partial\Omega \setminus (\Gamma_1 \cup \Gamma_2)$. We solve the forward problem using the continuous linear f nite element method and the exact data can obtain from the exact solution. To verify the issue of robustness and sensitivity for the reconstruction algorithm against the noise in the data, we introduce some multiplicative noise to the data z^δ along Γ_c in the time domain: $z^\delta = u + \delta\Re u \ \ on \ \ \Gamma_c \times (0,T)$, where $\Re$ a uniformly distributed random variable varying in $[-1,1]$, and δ is the noise level. We will apply $\delta = 5\%$ in our numerical tests unless specif ed otherwise. Assume that the regularization parameters $\beta = 10^{-4}$ and $\eta = 10^{-3}$ are chosen according to the theory of residues due to Morozov (see, [20]) and two tolerance parameters $\varepsilon_1 = \varepsilon_2 = 2\times10^{-3}$. Furthermore, we set the initial directions (d_q^0, d_γ^0) to be zeros vectors.

Now, we introduce five numerical examples for reconstructing the unknown parameters in the elliptic system (2.1), and assume that $\alpha(\mathbf{x}) = c(\mathbf{x}) = 1$. For example, we assume the exact solution for the forward problem (2.1) is given by

$$u(x, y) = x \cdot cos(\pi y) + y \cdot sin(\pi x),$$

Table 1 and Figs. 1, 2 present the convergence rate for the numerical solution of the forward problem. We assume that the source function for all examples is given by

$$f(\mathbf{x}) = (\pi^2 + 1)\cos(\pi y) + yx^2 - 3 \ \text{ in } \ \Omega,$$

and the boundary temperature is given by

$$g(\mathbf{x}) = \cos(\pi y + 1)\gamma(\mathbf{x}) + 2 \ \text{ on } \ \Gamma_1.$$

Remark 6.1. *The relative error of Robin coefficient is defined by* $\mathcal{RE}_\gamma = \frac{\|\gamma^k - \gamma\|_{L^2(\Gamma_1)}}{\|\gamma\|_{L^2(\Gamma_1)}}$ *and relative error of heat flux is defined by* $\mathcal{RE}_q = \frac{\|q^k - q\|_{L^2(\Gamma_2)}}{\|q\|_{L^2(\Gamma_2)}}$ *where the accuracy error is defined by the relative error.*

Example 6.1. *Consider the exact heat flux is given by* $q(\mathbf{x}) = -x + 3$ *on* Γ_2*, exact Robin coefficient* $\gamma(\mathbf{x}) = 2 - (y-1)^4$ *on* Γ_1*, and initial guess* $(\gamma^0, q^0) = (2, \frac{3}{2})$

- In this example we notice that the relative error of Robin coefficient decrease gradually with increasing the number of iterations and relative error of heat flux is regular with k.
- The obtained numerical results in Table 2 lead to the accuracy of the proposed algorithm for simultaneous reconstructing Robin coefficient and heat flux in Example 6.1.

Example 6.2. *Consider the heat flux is given by* $q(\mathbf{x}) = \frac{1}{2}(x-1)^2 + 2$ *on* Γ_2*, exact Robin coefficient is given by* $\gamma(\mathbf{x}) = \frac{3}{4}(y-1)^4 + \frac{5}{2}$ *on* $\{(x, y) \in \Gamma_1; 0 \le y \le 1\}$, $\gamma(\mathbf{x}) = \frac{-3}{4}(y-1)^4 + \frac{5}{2}$ *on* $\{(x, y) \in \Gamma_1; 1 \le y \le 2\}$*, and initial guess* $(\gamma^0, q^0) = (\frac{5}{2}, 2)$.

Fig.4 shows the exact and numerical reconstruction of Robin coefficient and heat flux such that $\mathcal{RE}_\gamma = 0.028$, $\mathcal{RE}_q = 0.0148$, and $k = 5$ at $\delta = 0.02$ noise in the data as shown in Table 2.

Example 6.3. *Consider the exact heat flux is given by* $q(\mathbf{x}) = -\frac{2}{5}(x-1)^2 + 2$ *on* Γ_2*. The exact Robin coefficient is given by* $\gamma(\mathbf{x}) = 1 + \frac{1}{5}(y-1)^2$ *on* Γ_1 *and initial guess is given by* $(\gamma^0, q^0) = (1, \frac{5}{2})$.

Fig.5 shows the exact and numerical reconstruction Robin coefficient and heat flux such that $\mathcal{RE}_\gamma = 0.0238$, $\mathcal{RE}_q = 0.0148$, and $k = 8$ at the noise level $\delta = 0.02$.

Example 6.4. *Consider the exact heat flux* $q(\mathbf{x}) = -x + 3$ *on* Γ_2*, the Robin coefficient is given by* $\gamma(\mathbf{x}) = 4 - (y-1)^2$ *on* Γ_1*, and the initial guess* $(\gamma^0, q^0) = (4, \frac{3}{2})$.

Fig.6 shows the behaviour and performance of γ and q with the exact solutions. In addition, the relative errors are given by $\mathcal{RE}_\gamma = 0.0257$, $\mathcal{RE}_q = 0.020$, and $k = 5$ at $\delta = 0.02$.

Example 6.5. *Assume that the exact heat flux is given by* $q(\mathbf{x}) = -x + 3$ *on* Γ_2*, the Robin coefficient is given by* $\gamma(\mathbf{x}) = 3 - (y-1)^4$ *on* $\{(x, y) \in \Gamma_1; 0 \le y \le 1\}$, $\gamma(\mathbf{x}) = 3 + (y-1)^4$ *on* $\{(x, y) \in \Gamma_1; 1 \le y \le 2\}$*, and initial guess* $(\gamma^0, q^0) = (3, \frac{3}{2})$.

By increasing the number of elements $\mathcal{N}_{el}$ and applying for any example such as Example 6.4. Then, we find that the numerical results in Table 4 and Fig. 7 are very stable and accurate. The numerical results show that the initial guess of Robin coefficient and heat flux depend on the given functions of $\gamma(\mathbf{x})$ and $q(\mathbf{x})$, respectively. Fig. 9 shows the numerical results for Example 6.1, such that decreasing the noise in the data gradually leads to increase the accuracy of the reconstruction heat flux and Robin coefficient accordingly. Table 2 declares that the proposed approach is convergent with respect to the noise in data for the all examples, this is more clearly seen in Figs. 9 and 10 for reconstructing the two parameters, simultaneously. The numerical reconstruction of the two parameters remain very steady and reasonable according to the noise level to 5%. We notice that, the results for the continuous functions are more accuracy about the discontinuous cases i.e. the smooth functions are adapted with the optimization problem (2.2). Tables 2 and 3 are presented to illustrate the efficiency and accuracy of the Levenberg-Marquardt method in addition to numerical convergence of the method. Fig. 11 shows the stability and accuracy of the modified conjugate gradient algorithm, such that the accuracy error decreases gradually with increasing the number of iterations.

Table 1: The convergence rate of the numerical solution of (2.1).

$\mathcal{N}_{el}$	$\mathcal{RE}_{sol}$
128	0.3121
512	0.1227
2048	0.0529
8192	0.0243
32768	0.0116
131072	0.0057

Table 2: Numerical results for the parameters identif - cation using MCGM and L-M method.

MCGM	δ	k	$\mathcal{RE}_\gamma$	$\mathcal{RE}_q$
Example 6.1	0.01	5	0.0146	0.0215
Example 6.2	0.01	4	0.0209	0.0217
Example 6.3	0.01	7	0.0139	0.0154
Example 6.4	0.01	5	0.0247	0.0185
Example 6.5	0.01	4	0.0135	0.0078
Example 6.1	0.02	5	0.0146	0.0216
Example 6.2	0.02	5	0.028	0.0148
Example 6.3	0.02	8	0.0238	0.0148
Example 6.4	0.02	5	0.0257	0.020
Example 6.5	0.02	3	0.0201	0.0109
L-M method	δ	k	$\mathcal{RE}_\gamma$	$\mathcal{RE}_q$
Example 6.1	0.01	14	0.0681	8.194e-004
Example 6.2	0.01	16	0.0387	0.0015
Example 6.3	0.01	12	0.0345	5.886e-004
Example 6.4	0.01	14	0.0391	0.0026
Example 6.5	0.01	17	0.0326	5.878e-004
Example 6.1	0.02	15	0.0676	6.763e-004
Example 6.2	0.02	16	0.0354	0.0015
Example 6.3	0.02	12	0.0416	7.213e-004
Example 6.4	0.02	14	0.0382	0.0027
Example 6.5	0.02	17	0.0330	5.371e-004

Table 3: Numerical results for the parameters identif cation at 3% and 5% noise in the data by **L-M method**.

Example	δ	k	$\mathcal{RE}_\gamma$	$\mathcal{RE}_q$	J
6.1	0.03	17	0.0688	5.84e-004	0.0856
6.2	0.03	17	0.0321	0.0016	0.0568
6.3	0.03	13	0.0505	8.36e-004	0.0418
6.4	0.03	14	0.0379	0.0028	0.0806
6.5	0.03	18	0.0350	5.00e-004	0.0846
6.1	0.05	35	0.0913	0.0021	0.1644
6.2	0.05	20	0.0317	0.0022	0.1183
6.3	0.05	38	0.1172	0.0031	0.0920
6.4	0.05	15	0.0381	0.0032	0.1553
6.5	0.05	20	0.0444	7.19e-004	0.1606

Table 4: Numerical results for Example 6.5 in the case of increasing the number of elements $\mathcal{N}_{el}$ by **MCGM**.

$\mathcal{N}_{el}$	k	$\mathcal{RE}_\gamma$	$\mathcal{RE}_q$	$\mathcal{N}_{el}$	k	$\mathcal{RE}_\gamma$	$\mathcal{RE}_q$
1408	4	0.024	0.007	614	5	0.028	0.008
1824	4	0.028	0.006	835	6	0.027	0.011
2584	5	0.02	0.017	998	5	0.028	0.011
3952	5	0.026	0.005	1184	6	0.025	0.01

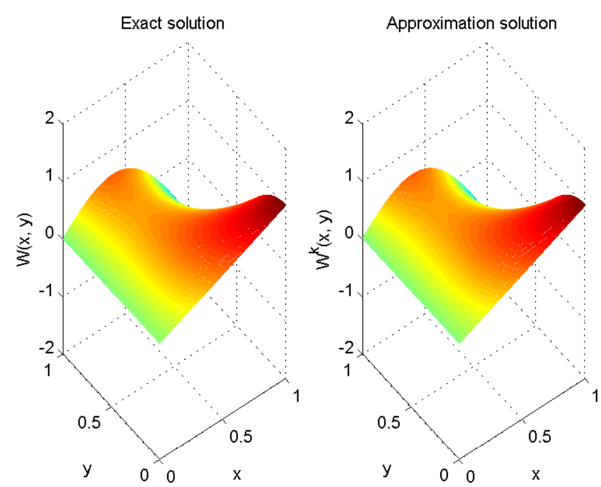

Figure 1: Exact solution (left) and numerical solution (right) with $\mathcal{N}_{el} = 131072$.

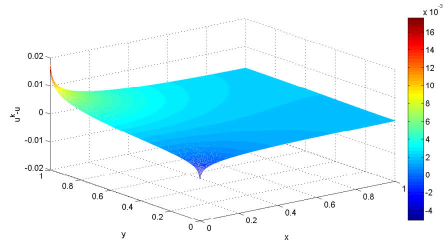

Figure 2: The difference between the exact and numerical solution for $u(x, y) = x \cdot cos(\pi y) + y \cdot sin(\pi x)$, $\mathcal{RE}_{sol} = 0.0057$.

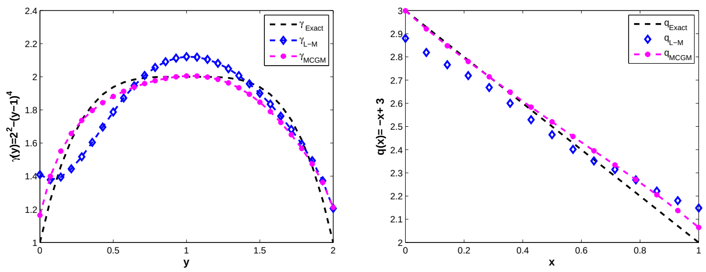

Figure 3: Exact and numerical reconstruction $\gamma(\mathbf{x})$ (left) and $q(\mathbf{x})$ (right) for Example 6.1 at $\mathcal{N}_{el} = 784$ by MCGM and L-M method.

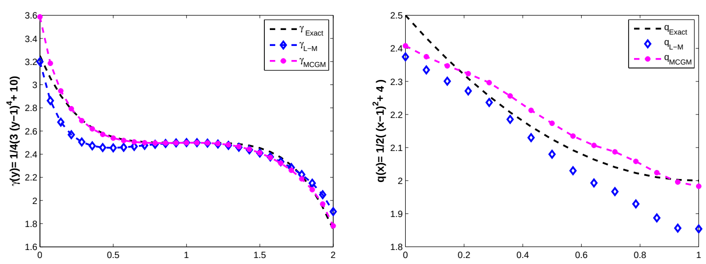

Figure 4: Exact and numerical reconstruction $\gamma(\mathbf{x})$ (left) and $q(\mathbf{x})$ (right) for Example 6.2 at $\mathcal{N}_{el} = 784$ by MCGM and L-M method.

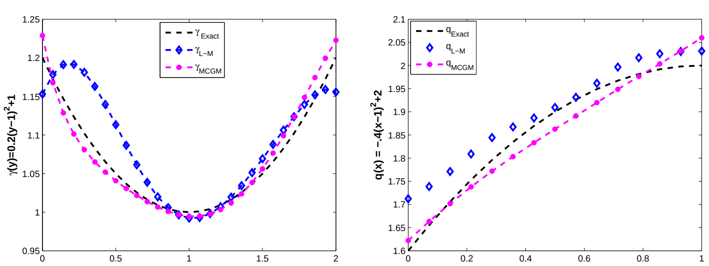

Figure 5: Exact and numerical reconstruction $\gamma(\mathbf{x})$ (left) and $q(\mathbf{x})$ (right) for Example 6.3 at $\mathcal{N}_{el} = 784$ by MCGM and L-M method.

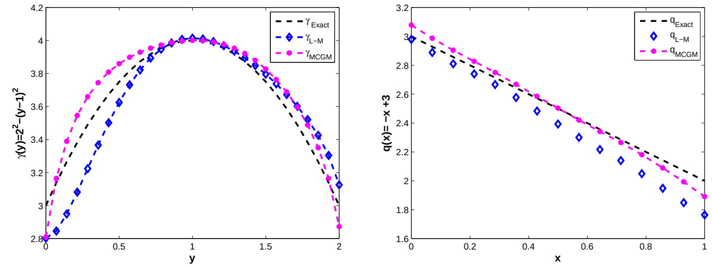

Figure 6: Exact and numerical reconstruction $\gamma(\mathbf{x})$ (left) and $q(\mathbf{x})$ (right) for Example 6.4 at $\mathcal{N}_{el} = 784$ by MCGM and L-M method.

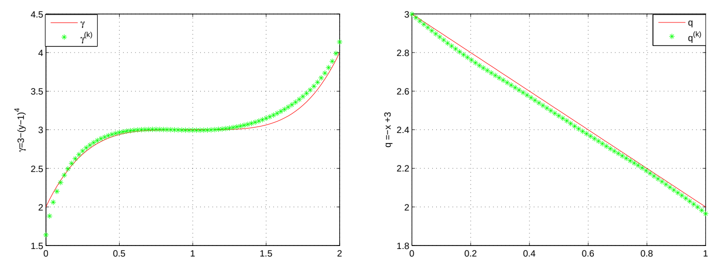

Figure 7: Exact and numerical reconstruction $\gamma(\mathbf{x})$ (left) and $q(\mathbf{x})$ (right) by Algorithm 5.1 for Example 6.5 at $N_{el} = 11840$ and $\delta = 0.02$.

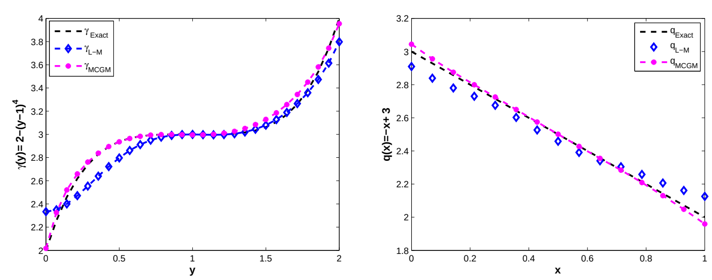

Figure 8: Exact and numerical reconstruction $\gamma(\mathbf{x})$ (left) and $q(\mathbf{x})$ (right) for Example 6.5 at $\mathcal{N}_{el} = 784$ by MCGM and L-M method.

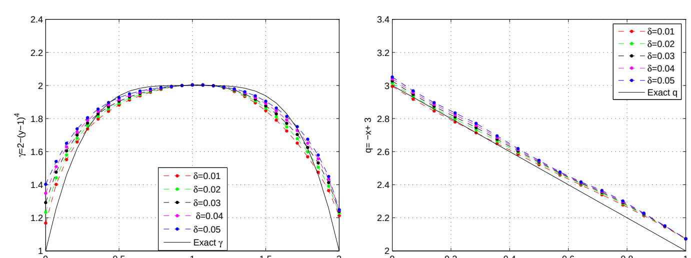

Figure 9: Exact and numerical reconstruction $\gamma(\mathbf{x})$ (left) and $q(\mathbf{x})$ (right) by Algorithm 5.1 for Example 6.1 with various levels of noise $\delta \in [0.01, 0.05]$.

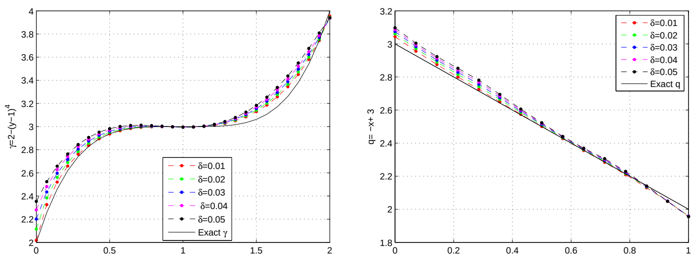

Figure 10: Exact and numerical reconstruction $\gamma(\mathbf{x})$ (left) and $q(\mathbf{x})$ (right) by Algorithm 5.1 for Example 6.5 with various levels of noise in the data $\delta \in [0.01, 0.05]$.

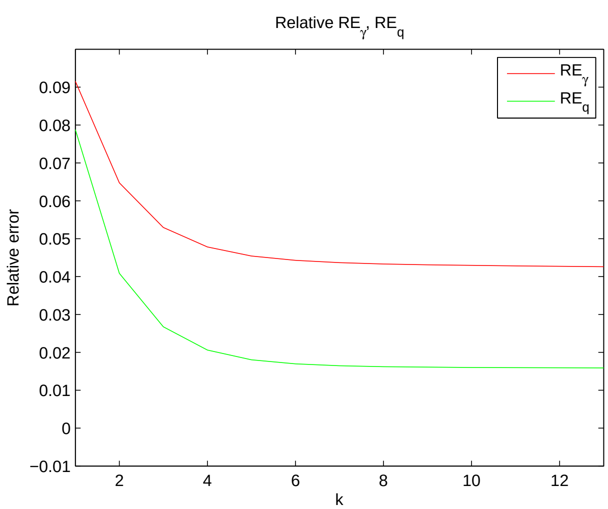

Figure 11: Convergence of the method for Example 6.1 with $\delta = 1\%$ noise in the data.

7 Concluding remarks

In this work, we studied the nonlinear inverse problem of simultaneous identifying the Robin coeff cient and heat f ux. We used the philosophy of the conjugate gradient method to simultaneous identifying two parameters. We derived the partial Fréchet derivatives of the forward solution to obtain the gradient formulas of the Robin coeff cient and heat f ux . Furthermore, introduced the adjoint equations to determine the step lengths. The f nite element approximation and its numerical and analysis convergence is investigated. We presented the numerical algorithm in details using the modif ed conjugate gradient method (MCGM) in addition to the idea of the modif cation. The foregoing numerical results and experiments with various levels of noise indicate that the proposed algorithm MCGM is very stable and eff cient for simultaneously reconstructing the two parameters heat f ux and Robin coeff cient. Moreover, they appear quite satisfactory in spite of the highly ill-posedness of the nonlinear inverse and discontinuity problem. We presented the numerical results by using Levenberg-Marquardt method with various levels of the noise to verify the robustness and eff ciency of the method. The comparison between the two methods MCGM and Levenberg-Marquardt methods in the work of [1] is investigated.

References:

[1] D. Jiang and T. A. Talaat, Simultaneous identif cation of Robin coeff cient and heat f ux in an elliptic system, International Journal of Computer Mathematics (2015) 1-12.

[2] D. Jiang, Y. Liu, M. Yamamoto, Inverse source problem for the hyperbolic equation with a time dependent principal part, Journal of Differential Equations 262 (1) (2017) 653-681.

[3] A. Tikhonov, V. Arsenin, Solutions of ill-posed problems wiley, New York 258.

[4] Y.-J. Yu, X.-L. Cheng, Numerical identif cation of Robin coeff cient by a KohnVogelius type regularization method, Inverse Problems in Science and Engineering (2016) 1-28.

[5] O. M. Alifanov, E. Artyukhin, A. V. Nenarokomov, Spline approximation of the solution of the inverse heat-conduction problem, taking account of the smoothness of the desired function, Teplof zika Vysokikh Temperatur 25 (4) (1987) 693-699.

[6] J. Beck, B. Blackwell, A. Haji-Sheikh, Comparison of some inverse heat conduction methods using experimental data, International Journal of Heat and Mass Transfer 39 (17) (1996) 3649-3657.

[7] B. Jin, J. Zou, Numerical estimation of piecewise constant Robin coefficient, SIAM Journal on Control and Optimization 48 (3) (2009) 1977-2002.

[8] G. Inglese, An inverse problem in corrosion detection, Inverse Problems 13 (4) (1997) 977-994.

[9] S. Chaabane, M. Jaoua, Identification of Robin coefficients by the means of boundary measurements, Inverse Problems 15 (6) (1999) 1425-1438.

[10] E. Sincich, Lipschitz stability for the inverse Robin problem, Inverse Problems 23 (3) (2007) 1311-1326.

[11] B. Jin, Conjugate gradient method for the Robin inverse problem associated with the laplace equation, International Journal for Numerical Methods in Engineering 71 (4) (2007) 433-453.

[12] L. Cheng, F. Zhong, H. Gu, X. Zhang, Application of conjugate gradient method for estimation of the wall heat flux of a supersonic combustor, International Journal of Heat and Mass Transfer 96 (2016) 249-255.

[13] B. Jin, J. Zou, Numerical estimation of the Robin coefficient in a stationary diffusion equation, IMA Journal of Numerical Analysis 30 (3) (2010) 677-701.

[14] F. Yang, L. Yan, T. Wei, The identification of a Robin coefficient by a conjugate gradient method, International Journal for Numerical Methods in Engineering 78 (7) (2009) 800-816.

[15] Y. L. Keung, J. Zou, Numerical identifications of parameters in parabolic systems, Inverse Problems 14 (1) (1998) 83-100.

[16] J. Xie, J. Zou, Numerical reconstruction of heat fluxes, SIAM Journal on Numerical Analysis 43 (4) (2005) 1504-1535.

[17] Y. F. Seid, J. Zou, Identifying parameters in elliptic systems by finite element methods with multi-level initializing techniques, Pitman Research Notes in Mathematics Series (1998) 213-228.

[18] I. Babuvška, W. C. Rheinboldt, Error estimates for adaptive finite element computations, SIAM Journal on Numerical Analysis 15 (4) (1978) 736-754.

[19] O. M. Alifanov, Inverse heat transfer problems, Springer Science & Business Media, 2012.

[20] V. Isakov, Inverse problems for partial differential equations, Vol. 127, Springer Science & Business Media, 2006.